A Review on the Migration Methods in B-scan Ground Penetrating Radar Imaging

Caner Özdemir[1, 2], **Sevket Demirci**[2], **and Enes Yiğit**[2]

[1]Department of Electrical and Electronics Engineering, Zirve University
Kızıllhisar Campus, Gaziantep 27260, Türkiye
[2]Department of Electrical-Electronics Engineering, Mersin University
Yenişehir, Mersin 33343, Türkiye

Abstract— Ground penetrating radar (GPR) has been a pioneering electromagnetic tool for detecting and locating subsurface objects with high imaging fidelities [1, 2]. The main defocusing effect in the GPR imagery is occurred due to the well-known hyperbolic distortion of the subsurface scatterers in the resultant space-time B-scan GPR image [1–3]. Although many migration/focusing methods have been proposed by various researchers, the focusing problem in the measured GPR images remains to be a challenging task. In this work, we review the recent migration methods of the B-scan GPR images that are popular among the GPR researchers. These methods are the hyperbolic summation (HS), the Kirchhoff migration, the $f-k$ migration and the SAR-based focusing techniques. The brief formulation of these methods together with their algorithms is presented. The applications of the algorithms to both the numerical and the measurement data are provided and the corresponding B-scan focused GPR images are presented.

1. INTRODUCTION

Ground Penetrating Radar (GPR) is a non-destructive remote sensing tool that is aimed to detect objects buried beneath the Earth's surface or situated interior to a visually opaque medium. In a typical space-time B-scan GPR image, any scatterer within the image region shows up as a hyperbola because of the different trip times of the EM wave while the antenna is moving along the B-scan path. Therefore, one of the most applied problem for the B-scan GPR image is to transform or migrate the unfocused space-time GPR image to a focused one showing the object's correct placement and size with its EM reflectivity. The common name for this task is called *migration* or *focusing* [4–6]. Kirchhoff wave-equation [4] and frequency-wave number ($\omega-k$) based [6, 7] migration algorithms are widely accepted and applied. The wave number domain focusing techniques; for instance, was first formulated for seismic imaging applications [6] and then adapted to the modern synthetic aperture radar (SAR) imaging practices [7]. These algorithms are also named as seismic migration and $\omega - k$ (or $f - k$) migration [8] by different researchers. In this paper, we present a brief review of the B-scan GPR migration/focusing methods that are commonly used by GPR research community.

2. MIGRATION TECHNIQUES

In this section, we will review the basic steps of the mostly applied GPR algorithms; namely hyperbolic summation (HS), the Kirchoff migration, $\omega - k$ (Stolt) migration and the SAR based focusing.

2.1. Hyperbolic (Diffraction) Summation

Let us assume a perfect point scatterer situated at (x_o, z_o) in the 2D plane where x-axis corresponds to the B-scan direction and the z-axis is the depth as illustrated in Figure 1. If the propagating medium is homogeneous, the parabolic hyperbola in the GPR image can be characterized by $\mathbf{R} = \sqrt{z_o^2 + (\mathbf{X} - x_o)^2}$ when the radar is moving on a straight path along X-axis. Here, $\mathbf{X}$ is the synthetic aperture vector along the B-scan and $\mathbf{R}$ represents the path length from the antenna to the scatterer. Assuming that the resultant B-scan GPR image can be regarded as the contribution of finite number of hyperbolas that correspond to different points on the object(s) below the surface, the following methodology can be applied to migrate the defocused image structures; i.e., hyperbolas to the focused versions:

1. For each pixel point; (x_i, z_i) in the 2D original B-scan space-depth GPR image; find the corresponding hyperbolic template using (1) and trace the pixels under this template.

2. Record the image data for the traced pixels under the template. This step provides 1D field data; $\mathrm{E^s}$ whose length; N is the same as the total number of sampling points in $\mathbf{X}$.
3. Then, take the root-mean-square (rms) value of the total energy contained within this 1D complex field data as follows:
4.

$$\{rms \text{ at } (x_i, z_i)\} = \sqrt{\frac{\left(|\mathbf{E^s}|^2 \, |(\mathbf{E^s})^*|^2\right)}{N}} = \frac{1}{\sqrt{N}} \sum_{i=1}^{N} |\mathbf{E_i^s}|^2 \tag{1}$$

5. The calculated rms value is recorded in the new GPR image at the point (x_i, z_i). This procedure is repeated until all pixels in the original GPR image are covered.

The concept of HS is illustrated through an example as shown in Figure 1. In this example, the measured data is collected from a subsurface scene where a thick iron pipe with 16.5 cm in diameter and 47 cm in length was buried flat about 15 cm below the ground. For the data collection, a stepped-frequency continuous radar (SFCWR) set-up by the help of vector network analyzer is utilized to measure the back-scattered field data along a straight line of discrete measurement points. The ground medium is occupied by dry and homogeneous sand. First, the classical space-depth B-scan GPR image is obtained by applying an IFT operation to the frequency domain back-scattered data as plotted in Figure 1(a). The major scattering from air-to-ground surface can be easily seen in the B-scan GPR image along the synthetic aperture direction for the depth of $z = 0$ m. The pipe below the surface manifests itself as a hyperbola in the image as expected. Second, we apply the methodology listed above for the hyperbolic summation realization of the GPR image. As depicted from the image in Figure 1(b), the hyperbolic defocusing is transformed to a more focused pattern in the migrated image.

2.2. Frequency-wavenumber (Stolt) Migration

The algorithm behind the frequency-wavenumber $(\omega - k)$ method works faster than the previously presented migration methods. Below is the brief explanation of the algorithm.

The algorithm begins with the 3D scalar wave equation for the wave function; $\varphi(x, y, z, t)$ within the constant-velocity propagation medium

$$\left(\frac{\partial^2}{\partial x^2} + \frac{\partial^2}{\partial y^2} + \frac{\partial^2}{\partial z^2} - \frac{1}{v_m^2}\frac{\partial^2}{\partial t^2}\right) \varphi(x, y, z, t) = 0 \tag{2}$$

In the Fourier space, spatial wave-numbers and the frequency of operation are related with the following equation

$$\varphi(x, y, z, t) = \left(\frac{1}{2\pi}\right)^{\frac{3}{2}} \iiint_{-\infty}^{\infty} E(k_x, k_y, \omega) e^{-j(k_x x + k_y y + k_z z - \omega t)} dk_x dk_y d\omega \tag{3}$$

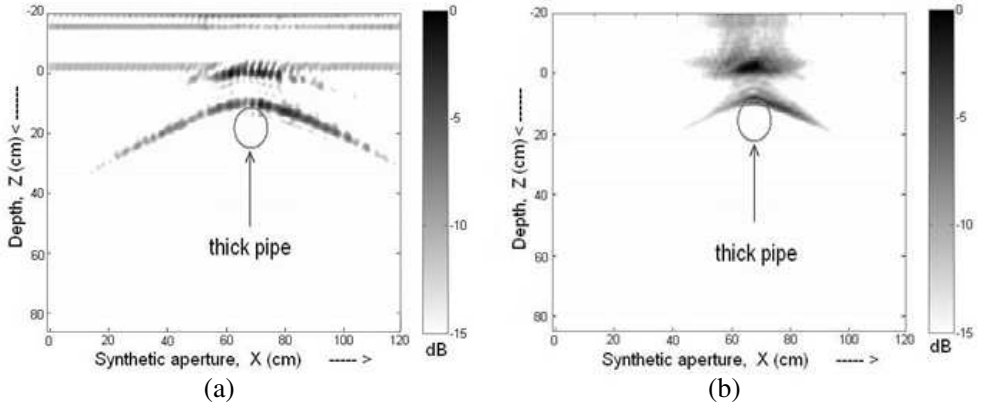

Figure 1: Measured B-scan GPR images: (a) hyperbolic B-scan image of a buried pipe, (b) focused image after applying the HS method.

For the GPR operation; the scattered field is taken to be measured on the $z = 0$ plane above the surface. When carefully treated, the above equation offers a Fourier transform pair where $e(x, y, t)$ can be regarded as the time-domain measured field on the $z = 0$ plane.

$$\varphi(x, y, 0, t) \triangleq e(x, y, t) = \left(\frac{1}{2\pi}\right)^{\frac{3}{2}} \iiint_{-\infty}^{\infty} E(k_x, k_y, \omega) e^{-j(k_x x + k_y y - \omega t)} dk_x dk_y d\omega \tag{4}$$

It is very important to notice that this equation designates a 3D forward FT relationship between $e(x, y, t)$ and $E(k_x, k_y, \omega)$ for the negative values of time variable; t. Then, the inverse FT can be dually defined as the following way:

$$E(k_x, k_y, \omega) = \left(\frac{1}{2\pi}\right)^{\frac{3}{2}} \iiint_{-\infty}^{\infty} e(x, y, t) e^{j(k_x x + k_y y - \omega t)} dx dy dt \tag{5}$$

Afterwards, we now use the ESM to focus the image by setting $t = 0$ in (4) and using

$$E(k_x, k_y, \omega) = e^{jk_z z} E(k_x, k_y, \omega,\ z = 0) \tag{6}$$

Therefore, one can get the time-domain measured field via

$$e(x, y, z, 0) = \left(\frac{1}{2\pi}\right)^{\frac{3}{2}} \iiint_{-\infty}^{\infty} E(k_x, k_y, \omega) e^{-j(k_x x + k_y y + k_z z)} dk_x dk_y d\omega \tag{7}$$

The above equation presents a focused image. However, the data in (k_x, k_y, ω) domain should be transformed to (k_x, k_y, k_z) domain to be able to use the FFT. Therefore, a mapping procedure from ω domain to k_z domain is required for fast processing. The relationship between the ω-and-k_z and $d\omega$-and-dk_z can be easily get as

$$e(x, y, z) = \left(\frac{1}{2\pi}\right)^{\frac{3}{2}} \iiint_{-\infty}^{\infty} \frac{v_m^2 k_z}{\omega} E^m(k_x, k_y, k_z) e^{-j(k_x x + k_y y + k_z z)} dk_x dk_y dk_z \tag{8}$$

Here $E^m(k_x, k_y, k_z)$ is the mapped version of the original data $E(k_x, k_y, \omega)$. After this mapping, the new data set does not lie on the uniform grid due to non-linear feature of the transformation. Therefore, an interpolation procedure should also be applied to be able to use the FFT for fast processing of the collected data set. The above focusing equation is valid for the 3D GPR geometry or the C-scan problem. Therefore, the focusing equation in (19) can be easily reduced to 2D B-scan GPR problem in the space-depth domain via the following equation:

$$e(x, z) = \left(\frac{1}{2\pi}\right) \iint_{-\infty}^{\infty} \frac{v_m^2 k_z}{\omega} E^m\left(k_x, k_z\right)\ e^{-j(k_x x + k_z z)} dk_x dk_z \tag{9}$$

2.3. SAR Based Focusing

In this work, we will present a SAR based focusing algorithm based on the plane wave decomposition of spherical wave-fronts in the 2D frequency-wavenumber domain. Assuming that the 2D scattered electric field $E^s(x, \omega)$ is recorded for different synthetic aperture points and frequencies for the B-scan GPR geometrical layout, the frequency domain back-scattered field from a point scatterer at r distance from the antenna will have the form of $E^s(\omega) = \rho \cdot e^{-j2\omega r/v_m}$ where $\omega = 2\pi f$ is the angular frequency, ρ is the strength of the scattered from the point target and v_m is the velocity of the wave. In the above equation, the propagation medium is assumed to be homogeneous. The number "2" in the exponential stands for the two-way propagation between the radar and the point scatterer on the object.

The general steps for SAR-based algorithm migration for the B-scan GPR operation can be summarized as the followings:

1. First, the scattered field data is collect the either in time domain to have $E^s(x, t)$ or in frequency domain to have $E^s(x, \omega)$.
2. Then, 2D FT of $E^s\left(x, t\right)$ or 1-D FT of $E^s(x, \omega)$ of taken to transform the data onto wave number–frequency plane to have $E^s(k_x, \omega)$. As demonstrated in [9], the data can be normalized as to be $\bar{E}_s(k_x, \omega)$.

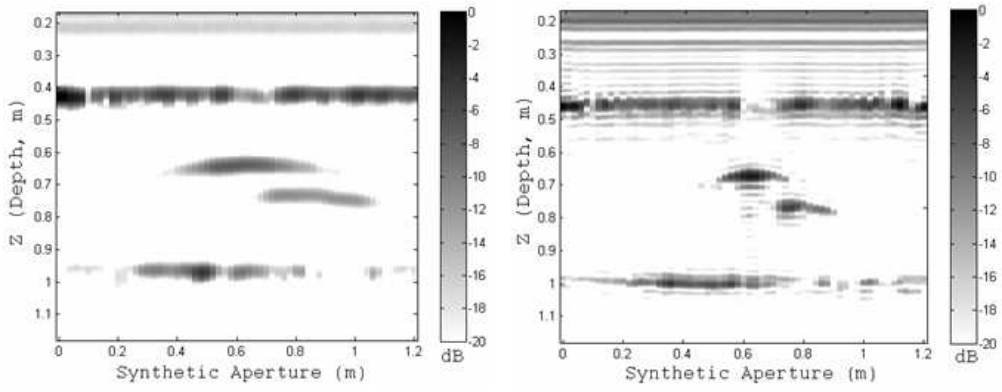

(a) (b)

Figure 2: Measured B-scan images of two closely placed pipes buried in sand (a) classical GPR image, (b) focused image after SAR based $\omega - k$ focusing.

3. In the next step, $\bar{E}_s(k_x, \omega)$ is mapped from $k_x - \omega$ domain to $k_x - k_z$ domain to transform the data spatial frequency domains to have $\tilde{E}^s(k_x, k_z)$.
4. In the final step, 2D IFFT of $\tilde{E}^s(k_x, k_z)$ is taken to get the final focused image in the Cartesian coordinates as $e^s(x, z)$.

An example of presented SAR based $\omega - k$ migration imaging algorithm is demonstrated through the results given in Figure 2. Two metal pipes that were buried flat around $z = 30\,\text{cm}$ and $z = 40\,\text{cm}$ in a dry and homogeneous sand environment as the geometry is seen in Figure 2(a). Using a vector network analyzer that can be used as stepped frequency continuous wave radar (SFCWR), a B-scan measurement was acquired along a straight path while the frequency is changed from 4.0 to 7.1 GHz. The classical space-depth B-scan GPR image is depicted in Figure 2(b) where the hyperbolic image distortion of the pipe responses can be clearly seen. Then, we apply the above presented SAR based $\omega - k$ migration algorithm in aiming to get a better focused image. The resultant migrated image is displayed in Figure 2(c) where the pipe responses are more localized around their correct locations.

3. CONCLUSION

In this paper, we have reviewed some fundamental algorithms for migrating the B-scan GPR data by presenting the algorithms steps of, HS, $\omega - k$ (Stolt) migration and SAR-based focusing algorithms. HS technique has been shown to be conceptually very simple to implement; but the computation time for completing the whole focusing procedure could be quite long if the image size is big. Stolt migration algorithm tries to constitute a 3D Fourier transform relationship between the image at the object space and the collected scattered field. Before applying FFT routine, a mapping procedure from frequency-wavenumber domain to wavenumber-wavenumber domain is needed. Although this mapping procedure may slow down the computation time, the algorithm is still fast thanks to the FFT step. SAR based focusing technique make use of the fact that the B-scan geometry is very similar to the stripmap SAR geometry. SAR based focusing algorithm also requires the same mapping in Stolt algorithm to be able to use two dimensional inverse FFT.

ACKNOWLEDGMENT

This work is supported by the Scientific and Research Council of Turkey (TUBITAK) under grant No: EEEAG-104E085.

REFERENCES

1. Daniels, D. J., *Surface-penetrating Radar*, IEE Press, London, 1996.
2. Peters, Jr., L., D. J. Daniels, and J. D. Young, "Ground penetrating radar as a subsurface environmental sensing tool," *Proc IEEE*, Vol. 82, No. 12, 1802–1822, 1994.
3. Ozdemir, C., S. Demirci, E. Yigit, and A. Kavak, "A hyperbolic summation method to focus B-Scan ground penetrating radar images: An experimental study with a stepped frequency system," *Microwave Opt. Tech. Letters*, Vol. 49, No. 3, 671–676, 2007.

4. Schneider, W. A., "Integral formulation for migration in two and three dimensions," *Geophysics*, Vol. 43, 49–76, 1978.
5. Gazdag, J., "Wave equation migration with the phase-shift method," *Geophysics*, Vol. 43, 1342–1351, 1978.
6. Stolt, R. H., "Migration by Fourier transform," *Geophysics*, Vol. 43, 23–48, 1978.
7. Cafforio, C., C. Prati, and F. Rocca, "Full resolution focusing of seasat SAR images in the frequency-wave number domain," *J. of Robotic Systems*, Vol. 12, 491–510, 1991.
8. Zhang, A., Y. Jiang, W. Wang, and C. Wang, "Experimental studies on GPR velocity estimation and imaging method using migration in frequency-wavenumber domain," *Proceedings ISAPE*, 468–473, Beijing, China, 2000.
9. Demirci, Ş, E. Yiğit, İ. H. Eskidemir, and C. Özdemir, "Ground penetrating radar imaging of water leaks from buried pipes based on back-projection method," *Independent Nondestructive Testing and Evaluation*, Vol. 47, 35–42, 2012.